Accepted Manuscript

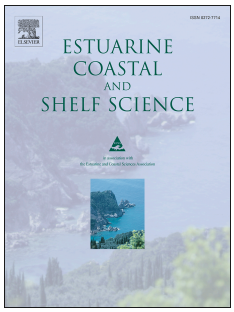

Uranium export from a sandy beach subterranean estuary in Australia

Christian J. Sanders, Isaac R. Santos, Mahmood Sadat-Noori, Damien T. Maher, Ceylena Holloway, Bernhard Schnetger, Hans-J. Brumsack

PII: S0272-7714(17)30384-0

DOI: 10.1016/j.ecss.2017.09.002

Reference: YECSS 5604

To appear in: *Estuarine, Coastal and Shelf Science*

Received Date: 10 April 2017

Revised Date: 28 August 2017

Accepted Date: 2 September 2017

Please cite this article as: Sanders, C.J., Santos, I.R., Sadat-Noori, M., Maher, D.T., Holloway, C., Schnetger, B., Brumsack, H.-J., Uranium export from a sandy beach subterranean estuary in Australia, *Estuarine, Coastal and Shelf Science* (2017), doi: 10.1016/j.ecss.2017.09.002.

Uranium export from a sandy beach subterranean estuary in Australia

Christian J. Sanders*[1], Isaac R. Santos[1,2], Mahmood Sadat-Noori[1,2], Damien T. Maher[2], Ceylena Holloway[1,] Bernhard Schnetger[3], Hans-J. Brumsack[3]

[1] National Marine Science Centre, Southern Cross University, PO Box 4321, Coffs Harbour, NSW 2450, Australia

[2] School of Environment, Science and Engineering, Southern Cross University, PO Box 157, Lismore, NSW 2480, Australia

[3] Institute for Chemistry and Biology of the Marine Environment (ICBM), Carl-von-Ossietzky University Oldenburg, D-26111 Oldenburg, Germany

Corresponding author: ***christian.sanders@scu.edu.au**

Running head: dissolved uranium in coastal groundwater

Key words: coastal groundwater; estuarine chemistry; uranium, subterranean estuary; ocean budget

ABSTRACT

Few studies exist on the contribution of subterranean estuaries (STEs) to the oceanic uranium (U) budget. Here, we estimate the dissolved U fluxes out of a quartz sand STE located on the east coast of Australia. Our results indicate that the advective flow of seawater in permeable sands enhances cycling of U in the STE. Dissolved U concentrations ranged from 25 nM in the STE to an effective zero salinity end-member of 3.8 nM in the surface estuary. The dissolved U (salinity corrected) concentrations were positively correlated to Fe (r^2 = 0.49 $p < 0.001$) during a shallow beach time series experiment. These results indicate that reductive dissolution of Fe oxides may be an important process maintaining high concentrations of U in shallow permeable sand STEs. The U export rates from the STE to the surface estuary in this study were estimated to be 1.8 µmol U m^{-2} day^{-1} based on the shallow saline groundwater exchange pathways and 0.4 µmol U m^{-2} day^{-1} based on the deep fresh submarine groundwater discharge (SGD). Uranium's behavior in STEs is diverse and site specific. Out of the seven investigations available here and in the literature, three suggested a SGD-derived U source to the coastal ocean, while four suggested a U sink within STEs removing seawater U. Therefore, it remains unclear whether SGD is a source or sink of U to the ocean and additional investigations in contrasting settings are required to resolve the global contribution of SGD to the marine U cycle.

1. Introduction

Subterranean estuaries (STE) are located in geochemically dynamic transition zones, where fresh groundwater and seawater mix (Moore, 1999; Roy et al., 2010). The STE and coastal groundwater are a known source of several important solutes including nutrients, carbon, and trace metals to the coastal ocean (Moore, 1999; Sanders et al., 2012). Recent studies indicate that due to dynamic geochemical processes associated with groundwater – seawater interactions, STE's may be important to oceanic uranium (U) budgets (Charette and Sholkovitz, 2006; Dunk et al., 2002). Tidal pumping and fresh water fluxes along the STE drive the highly dynamic trace metal precipitation and dissolution cycles which are underpinned by oscillating redox conditions that are difficult to characterize (Gonneea et al., 2008; Gonneea et al., 2013a; Klinkhammer and Palmer, 1991; Moore, 2008; Rodellas et al., 2014; Roy et al., 2013; Roy et al., 2012; Sanders et al., 2012; Santos et al., 2008; Santos et al., 2010).

The dissolved U concentration in the ocean is approximately 13.6 nM with river inputs of 3 to 5 x 10^7 mol U $year^{-1}$ (Andersen et al., 2016; Chen et al., 1986; Owens et al., 2011). In general, U shows a distinct non-conservative behavior in tidal estuaries (Anderson, 1987). While fresh subterranean groundwater discharge (SGD) is expected to be a source of U, saline SGD creates conditions for the removal of seawater U by some aquifer materials (Moore et al., 2011). As such aquifer lithology plays a major role in whether STEs are a U source or sink to the coastal ocean (Gonneea et al., 2014). For example, investigations in karst aquifers have shown that U is released into solution in the STE and represent a source to the ocean (Gonneea et al., 2014; Swarzenski and Baskaran, 2006), while other studies in estuarine sands and saltmarsh settings have indicated that STEs are U sinks (Beck et al., 2008; Charette and Sholkovitz, 2006; Moore et al., 2011; Santos et al., 2011).

Previous studies have also highlighted gaps in the U oceanic budgets of which STEs may play important roles (Dunk et al., 2002). The source or sink behavior of U in STEs is a function of not only the aquifer lithology but other geochemical properties, including redox conditions as well as the proportion of fresh versus saline SGD (Swarzenski, 2007; Swarzenski and Baskaran, 2006). For instance, under oxic conditions, U is more soluble and can be released to solution, while under anoxic conditions U is less soluble and may be adsorbed on particles. Uranium carbonate complexation and pH are also important geochemical parameters which influence dissolution or precipitation (Langmuir, 1978). A better understating of the source or sink processes that drive the global U budgets can provide pivotal understanding of specific processes such as historical changes in marine ocean water chemistry (Andersen et al., 2015; Tissot and Dauphas, 2015). However, the current lack of data in different environmental conditions prevents a reliable assessment of whether SGD may play a major role in the oceanic U budget.

The objective of this work is to investigate U behavior and fluxes in a quartz sand STE during a tidal cycle as well as along vertical and horizontal transects. Iron, Mn, Ba, DOC, pH, salinity, DO% were also analyzed to assist in explaining the dissolved U behavior along the STE. We attempt to determine the source or sink behavior of U in the STE by estimating deep fresh groundwater fluxes and shallow saline groundwater fluxes to the surface estuary.

2. Methods

Field measurements were undertaken in a quartz sand beach STE, near a coastal estuarine creek, located in Hat Head, New South Wales, Australia (153°3'27.268"E, 31°3'24.801"S) (Figure 1). The coastal creek in this study (Korogorro Creek) has a catchment area of approximately 18 km^2. The creek is tidally flushed (Acworth et al., 2007) with salinity ranging

93 from 5 to 35 ppt at the mouth of the creek (Sanders et al., 2015). The bedrock is found at depths
94 between 60 to 80 m and permeable quartz sands characterize the tidal estuary with depths of up
95 to 30 m (Acworth et al., 2007). A combination of silty sands, silts and clays lie beneath the upper
96 sandy region. The region has an average annual precipitation of 1,490 mm and has a subtropical
97 climate (http://www.bom.gov.au). The U dataset reported here builds on recent radon and radium
98 isotope (Sadat-Noori et al., 2015) and dissolved Fe (Sanders et al., 2015) investigations at the
99 same site.

100 A total of 84 groundwater and 59 surface water samples were collected from different
101 locations (Figure 1) following four different approaches: (1) a vertical groundwater profile at the
102 low tide mark approximately every ~2 hours for almost 12 hours, from 0.5 to 2.7 m depths
103 (hereafter referred to as beach time series) to cover a complete tidal cycle (39 samples), (2) a 2
104 dimensional groundwater transect along the beach hereafter referred to as 2D transect (18
105 samples) (distance measured from the landward station to the seaward edge (m)) using a push
106 point piezometer system as described elsewhere (Charette and Allen, 2006), (3) groundwater
107 sampling from permanent monitoring deep wells and shallow piezometers, spatially distributed
108 in the catchment (27 samples), and (4) surface estuarine water time series samples during the
109 summer (wet season) and winter (dry season) at 1 hour time steps over 30 hours (59 samples) as
110 originally reported by Sanders et al. (2015). Water samples were analyzed for dissolved metals
111 and dissolved organic carbon (DOC) along with physicochemical parameters. The wells in this
112 work were dug in the intertidal zone at low tide. Screened PVC pipes were installed to allow
113 groundwater infiltration (De Weys et al., 2011). A peristaltic pump was used to collect samples
114 after the wells were purged at least 3 volumes. A calibrated handheld YSI was used to determine
115 pH, temperature, DO and salinity for each sample. While all the groundwater U data is unique to

116 this study, other observations for the surface water time series measurements are presented in
117 Sanders et al. (2015). Groundwater times series, 2D transect and shallow bore samples were
118 collected in the wet season and groundwater deep samples were collected in the dry season.

119 Dissolved Ba, Fe, Mn, Mo and U were measured by a magnet sector high resolution ICP-MS
120 (Element II, Thermo-Fisher) at the ICBM using internal standards (^{115}In for ^{138}Ba and ^{238}U, ^{89}Y
121 for ^{56}Fe and ^{55}Mn) and a dilution factor of 20 for samples with a salinity of 35 (or lower if
122 salinity was lower). Samples could not be measured with the same dilution factor because the
123 salinity ranged from 0-35. To avoid matrix effects during measurement by ICP-MS salt content
124 was diluted to < 0.2%. Ba and U were measured in low resolution (300) and Fe and Mn in
125 medium resolution (4500). Precision for all isotopes was better than 5%, except for Mn in some
126 samples below 50 nM where precision was in the 5-10% range. Accuracy was checked by
127 several seawater reference materials (CASS-5 and NASS-5, NASS-6, NRC Canada). Accuracy
128 for Mn in the CRM´s (9- 48 nM level) was better than 8%. As some samples for Mn and all
129 samples for Fe were much higher than in the CRM´s, we also spiked the CRM´s; in these CRM´s
130 accuracy was better than 4%. Ba was measured in CASS-5 resulting in 53±2 nM, (n=64) which
131 is close to our ICP-OES measurements (51 ±5 nM, n=44) (both mean of 3 years). For U, a
132 salinity derived concentration for U was assumed if no certified value was given, and agreement
133 was within 6%. Uranium reference values are from the National Research Council Canada
134 (NRCC). DOC was analyzed using the wet oxidation method with an OI Analytical 1030W TOC
135 analyzer following the methods described in detail elsewhere (Maher and Eyre, 2010). DOC
136 standards analyses were made of potassium hydrogen phthalate (KHP), and analytical precision
137 was better than 2%.
138

Results

The dissolved U concentrations were highest in the 2D groundwater transect, 25.3 nM (1 m depth and 12.6 meters from the seaward edge) (Supplementary Material). During the shallow beach time series measurements, dissolved U values reached 22.9 nM, while the highest concentrations in the deep groundwater were 0.6 nM. The dissolved U concentrations in the surface estuary were up to 13.5 nM (Sanders et al., 2015) which is similar to the average oceanic concentration of 13.6 nM (Andersen et al., 2016; Chen et al., 1986; Owens et al., 2011).

3.1 Beach time series

The shallow beach time series (0.5 to 2.7 m depth) measurements showed tidal fluctuations in dissolved metal concentrations (Figure 2). The U, Fe and Mn concentrations were highest during the ebbing and low tides, up to 22.9 nM, 15900 nM, and 328 nM respectively, while Ba concentrations were highest during the flood tide (up to 112 nM). Dissolved organic carbon concentrations showed the highest concentrations at the 1.5 m depth during high tide, up to 544 µM. The pH was higher at low tide and towards the surface of the STE, up to 8.1, and lowest towards the 2.7 m depth, reaching 7.9. During the times series measurement, salinities ranged from 17.9 to 33.3 (Figure 2).

3.2 Two dimensional (2D) transect

The 2D groundwater observations showed differing site specific metal hotspots along the STE (Figure 3). The dissolved U concentrations were highest towards the center of the STE, while salinity was highest in the seaward most station and at the surface, up to 33.3, and DOC was highest (629 µM) towards the landward most station. Dissolved Fe concentrations were highest at the surface, up to 10900 nM and towards the center of the STE, while Mn concentrations were highest towards the landward most station, up to 375 nM. Barium

concentrations peaked at the surface near the center stations of the STE where saltwater first contacts fresh groundwater within the STE, up to 72.8 nM) (Supplementary Material).

3.3 Shallow and deep wells

The dissolved U concentrations were lowest in the deep wells, reaching a maximum of 0.6 nM at the 18 m depth, and below the detection limit at most of the other deep well sites (Supplementary Material). In the shallow wells, U concentrations reached 15.7 nM at the 1.5 m depth. The Fe concentrations at the 4 m depth in shallow beach groundwater were 13000 nM and increased at the 6 m depth in the deep groundwater station up to 16700 nM. Dissolved Mn concentrations were highest at the 1.5 m depth of the shallow groundwater station (858 nM) and up to 4470 nM at the 7.5 m of the deep groundwater station. Dissoved Ba concentrations were highest at the 1.5 m depth (813 nM) in shallow beach groundwater and highest at the 7.5 m depth in the deep groundwater station, concentrations up to 164 nM. DOC peaked at 7730 uM, at the 2.7 m depth of the shallow groundwater station and reached 10200 uM at the 6.0 m of the deep groundwater station (Supplementary Material).

3.4 Surface water U distributions

The surface estuary U concentrations show a positive relationship to salinity, being highest during high tide, with a similar concentration range during both times series experiments of 12.9 to 2.6 (winter/dry) and 12.8 to 1.7 nM (summer/wet) (Sanders et al., 2015). The dissolved U concentration in ocean water is approximately 13.6 nM at 35 ppt salinity (Chen et al., 1986). All other parameters had similar tidal trends.

3. Discussion

184 The large salinity fluctuations within the STE, from 17.9 at low tide to 33.3 at high tide,
185 during the beach time series measurements (Figure 2) demonstrate effective flushing of the
186 beach sands. While two hours after high tide there was an obvious injection of freshwater, with
187 salinity dropping from 33.3 to 20.1, there was an equally important salinity increase (from 20.1
188 to 24.9) following low tide. Each of these water sources have differing U concentrations. In
189 seawater, U is conservative in its soluble state U^{+6}, and stable when complexed with carbonates,
190 thus increasing its mobility (Koide and Goldberg, 1963). However, when anoxic conditions
191 prevail, U^{+6} is reduced to U^{+4}, decreasing its solubility and binding to DOC, humic acids and
192 other forms of organic material (Carroll and Moore, 1993; Dosseto et al., 2006; Klinkhammer
193 and Palmer, 1991). Dissolved U can be removed from solution to solid phases in the presence of
194 Fe and Mn (hydr)oxides, for which U has a relatively strong affinity, forming oxide precipitates
195 in subterranean estuaries (Cochran et al., 1986). It is apparent that U precipitation processes are
196 occurring at the onset of high tide in the STE, as indicated in the time series beach experiment,
197 when the dissolved U concentrations decline to 5 nM at the peak of high tide (Figure 2),
198 followed by U release as lower salinity, higher pH water dominates the STE during the falling
199 tide.

200 The 2D transect as well as the shallow and deep groundwater samples indicate that the
201 dissolved U concentrations did not directly correlate to other trace metals, depth, DOC, salinity
202 or pH (Figure 4) . However, the U concentrations were positively correlated to Fe during the
203 beach time series measurements ($R^2 = 0.46$ $p < 0.001$) (Figure 4). Salinity corrected U values
204 (U/sal ratios), used to correct for simple dilution effects, were also positively correlated to Fe
205 during beach time series measurements ($R^2 = 0.49$ $p < 0.001$) (Figure 5). No relationship was
206 found between the dissolved Mn and U concentrations even though Mn oxides may also be

strong U absorbers (Goldberg, 1954) (Figure 4). This is likely related to the differences in Fe and Mn oxidation and reduction properties (Burdige, 1993).

The time series measurements are of interest here because trace metal dissolution-precipitation/sorption-desorption cycles are noted in relation to the tidal movement. Indeed, the dynamic, non-conservative behavior of dissolved U is noted from the U vs salinity distributions during the groundwater observations (Figure 6). These results indicate that the dissolved U concentrations may be driven by differing geochemical processes such as redox cycling along the STE, as the reductive dissolution of Fe oxides may be an important process in maintaining high concentrations of U in the shallow beach groundwater (up to 22.9 nM). As Fe (hydr)oxides are strong absorbers of dissolved U, Fe may come into solution under reducing conditions and release trace metals such as U (Charette and Sholkovitz, 2002). In the quartz sand beach STEs of this work, the freshwater-seawater boundary appears to have a significant impact on oxidative precipitation of groundwater U and Fe, i.e. the 'iron curtain effect'(Charette and Sholkovitz, 2002).

During the ebb, low and flood tides, concentrations of Fe and U were greater at depths slightly above 1.5 m (Figure 2). This suggests that as tidal oxic surface and bottom waters infiltrate the upper and lower STE, redox processes confine the dissolved U and Fe towards the 1.5 m depth of the STE (Figure 2). Studies in the Waquoit Bay (Cape Cod, Massachusetts, USA) also showed vertical stratification of U, with concentrations reaching 27 nM, in a region of the STE subject to redox cycles (Charette and Sholkovitz, 2006; Charette et al., 2005). However, here, the U-salinity distributions in the higher salinity samples from the surface estuary resulted in an effective zero salinity end-member concentration of 3.8 nM (Figure 6), In contrast, Charette and Sholkovitz (2006) found a zero salinity end-member of -5.7 nM using surface water

samples influenced by SGD. Hence, in this work, extrapolating the surface estuary U trend back to the zero salinity intercept yields a source of dissolved U, while in Waquoit Bay a sink was implied (Charette and Sholkovitz, 2006). Other studies in North America (Duncan and Shaw, 2003; O'Connor et al., 2015; Santos et al., 2011) and Europe (Moore et al., 2011) found STEs to be sinks by extrapolating the U trend in STE groundwaters or surface waters back to the zero salinity, while studies in carbonate systems in South Florida and Yucatan Mexico dominated by fresh SGD found STEs to be a source of U to the ocean (Gonneea et al., 2014; Swarzenski and Baskaran, 2006) (Table 1).

We estimate SGD derived U fluxes using two approaches. We first use Charette and Sholkovitz's (2006) approach to determine the effective SGD endmember. This approach relies on the zero salinity intercept using surface water samples only (3.8 nM; see Figure 6) and assumes that U cycling within the estuary is driven primarily by seawater recirculation in sediments. Using the total SGD rate of 469 L m^{-2} d^{-1} (Sadat-Noori et al.; 2015), this approach results in a U flux of 1.8 μmol m^{-2} d^{-1}. A second approach ignoring seawater recirculation in sediments can be estimated by simply multiplying the fresh SGD rate (275 L m^{-2} d^{-1}) by the average U concentration in fresh groundwater (1.5 nM in all 23 samples with salinity <2), resulting in fluxes of 0.4 μmol m^{-2} d^{-1}. This second approach ignores any U transformations in the subterranean estuary, and may represent the long term flux of new terrestrial U via SGD assuming that periodic sorption/desorption cycles of seawater U within the STE result in no net long term flux. Therefore, we suggest that the U fluxes are most likely between 0.4 and 1.8 μmol m^{-2} d^{-1}.

Regardless of assumptions involved in these calculations, these SGD-derived U fluxes are positive and greater than what was found from the karst sediments in the Yucatan and in South

Florida (Gonneea et al., 2014; Swarzenski and Baskaran, 2006) (Table 1). Furthermore, the U export rates in this study are in contrast to research that suggest that STEs are U sinks (Charette and Sholkovitz, 2006; De Weys et al., 2011; Duncan and Shaw, 2003; Moore et al., 2011; O'Connor et al., 2015; Santos et al., 2011; Windom and Niencheski, 2003) (Tables 1). For instance, Charette and Sholkovitz (2006) found U removal rate of -0.4 μmol m^{-2} d^{-1} on the northeastern coast of North America and Santos et al. (2011) reports that STEs removal of U at -1 μmol m^{-2} d^{-1} on the northern coast of the Gulf of Mexico (Table 1). Comparing these solute fluxes via SGD should be made with care because of differences in the spatial scale of sampling (Bratton, 2010). For example, while the Yucatan investigation represents a large continental shelf (~2 km wide, ~1100 km long), our investigation covers a much smaller scale within an estuary ~20 m wide and ~5 km long. The SGD chemical signal in small spatial scale investigations is likely to be stronger than in large scale investigations (Bratton, 2010).

We use the data in this work and that available in the literature to update first order estimates of the global contribution of SGD to the marine U budget. Using the global estimates of fresh SGD from Burnett et al. (2003) of 4,000 to 100,000 km^3 y^{-1}, and the average effective U endmember in SGD from the seven systems in Table 1 (-13.4 nM), the U export rates from SGD would be negative at -5.4×10^7 to -1.3×10^9 mol y^{-1} (Table 2). In this case, SGD would be interpreted as a sink of dissolved U. The average SGD endmember is highly influenced by the Turkey Point outlier at -119 nM (Table 1). Omitting Turkey Point results in an average U endmember of 1.7 nM which would lead to the interpretation of SGD as a source of U to the oceans at 6.8×10^6 to 1.7×10^8 mol y^{-1} (Table 2). The seven independent studies shown on Table 1 show large variations in the U fluxes. Therefore, global extrapolations may not adequately account for the complex U cycling in geologically diverse STEs. The very wide range in all of

these SGD estimates falls in a comparable order of magnitude of estimates of global river inputs and saltmarsh removal of U (Table 2). Upscaling of SGD U export rates to a global scale has large uncertainties associated with poorly known temporal and spatial variability and a substantial variability in physical and geochemical differences amongst coastal areas. Furthermore, the results in these studies are based on single sampling campaigns which may not reflect the STE dynamics on a seasonal scale (Gonneea et al., 2013a). For instance, investigations focusing on radium isotopes and barium reveal a strong seasonal cycles related to storage and release cycles that control the timing of SGD fluxes (Gonneea et al., 2013b). For these reasons, we feel that the current research is not mature enough to provide SGD-derived U fluxes to the global ocean, and additional investigations in diverse settings would be required to better constrain the contribution of SGD to the marine U budget.

4. Conclusion

This study compares the dissolved U fluxes in a range of lithology diverse STEs to establish a more detailed view into the geochemical cycling of U in coastal aquifers. The shallow beach groundwater measurements in this and in previous studies indicate that these systems are highly dynamic in the site specific STEs around the globe. The large differences in U flux rates in this and in previous studies, acting as sinks in North America and Europe while a source in karst sediments (South Florida, Central America) and sandy beaches of Australia, indicates that a combination of physical and geochemical processes control U cycling in STEs. The highly permeable quartz sand STEs in this region of Australia sustains the reductive dissolution of Fe (hydr)oxide along with tidal pumping which may drive U export rates. A first order upscaling exercise relying on the seven available estimates (4 systems were a sink for U, and 3 were a

299 source of U) implies that SGD may be either a major sink or major source of U to the ocean
300 depending on assumptions made. More comprehensive estimates are needed in differing regions
301 to better constrain the U behavior is STEs and the contribution of SGD to global U budgets.
302
303 **Acknowledgments**
304 Field investigations were funded by the Australian Research Council (ARC; DP120101645) and
305 an ARC DECRA to CJS (DE160100443). DTM acknowledges funding from the ARC
306 (DE150100581). We would like to thank Luciana Sanders, Paul Macklin, Ashley McMahon,
307 Benjamin Stewart, Jennifer Taylor, and Judith Rosentreter for their support during field
308 campaigns. We acknowledge constructive comments by two anonymous reviewers that
309 significantly improved the manuscript.
310
311 **References**
312
313 Acworth, R.I., Hughes, C.E., Turner, I.L., 2007. A radioisotope tracer investigation to determine
314 the direction of groundwater movement adjacent to a tidal creek during spring and neap
315 tides. Hydrogeology Journal 15, 281-296.
316 Andersen, M.B., Elliott, T., Freymuth, H., Sims, K.W.W., Niu, Y., Kelley, K.A., 2015. The
317 terrestrial uranium isotope cycle. Nature 517, 356-359.
318 Andersen, M.B., Vance, D., Morford, J.L., Bura-Nakić, E., Breitenbach, S.F.M., Och, L., 2016.
319 Closing in on the marine 238U/235U budget. Chemical Geology 420, 11-22.

320 Beck, M., Dellwig, O., Schnetger, B., Brumsack, H.J., 2008. Cycling of trace metals (Mn, Fe,
321 Mo, U, V, Cr) in deep pore waters of intertidal flat sediments. Geochimica et
322 Cosmochimica Acta 72, 2822-2840.
323 Burdige, D.J., 1993. The biogeochemistry of manganese and iron reduction in marine sediments.
324 Earth Science Reviews 35, 249-284.
325 Carroll, J., Moore, W.S., 1993. Uranium removal during low discharge in the Ganges
326 Brahmaputra mixing zone. Geochimica et Cosmochimica Acta 57, 4987-4995.
327 Charette, M.A., Allen, M.C., 2006. Precision ground water sampling in coastal aquifers using a
328 direct-push, shielded-screen well-point system. Ground Water Monitoring and
329 Remediation 26, 87-93.
330 Charette, M.A., Sholkovitz, E.R., 2002. Oxidative precipitation of groundwater-derived ferrous
331 iron in the subterranean estuary of a coastal bay. Geophysical Research Letters 29, 85-81.
332 Charette, M.A., Sholkovitz, E.R., 2006. Trace element cycling in a subterranean estuary: Part 2.
333 Geochemistry of the pore water. Geochimica et Cosmochimica Acta 70, 811-826.
334 Charette, M.A., Sholkovitz, E.R., Hansel, C.M., 2005. Trace element cycling in a subterranean
335 estuary: Part 1. Geochemistry of the permeable sediments. Geochimica et Cosmochimica
336 Acta 69, 2095-2109.
337 Chen, J.H., Lawrence Edwards, R., Wasserburg, G.J., 1986. 238U, 234U and 232Th in seawater.
338 Earth and Planetary Science Letters 80, 241-251.
339 Cochran, J.K., Carey, A.E., Sholkovitz, E.R., Surprenant, L.D., 1986. The geochemistry of
340 uranium and thorium in coastal marine sediments and sediment pore waters. Geochimica
341 et Cosmochimica Acta 50, 663-680.

342 De Weys, J., Santos, I.R., Eyre, B.D., 2011. Linking groundwater discharge to severe estuarine
343 acidification during a flood in a modified wetland. Environmental Science and
344 Technology 45, 3310-3316.
345 Dosseto, A., Turner, S.P., Douglas, G.B., 2006. Uranium-series isotopes in colloids and
346 suspended sediments: Timescale for sediment production and transport in the Murray
347 Darling River system. Earth and Planetary Science Letters 246, 418-431.
348 Duncan, T., Shaw, T.J., 2003. The mobility of Rare Earth Elements and Redox Sensitive
349 Elements in the groundwater/seawater mixing zone of a shallow coastal aquifer. Aquatic
350 Geochemistry 9, 233-255.
351 Dunk, R.M., Mills, R.A., Jenkins, W.J., 2002. A reevaluation of the oceanic uranium budget for
352 the Holocene. Chemical Geology 190, 45-67.
353 Goldberg, E.D., 1954. Marine Geochemistry 1. Chemical Scavengers of the Sea. The Journal of
354 Geology 62, 249-265
355 Gonneea, M.E., Charette, M.A., Liu, Q., Herrera-Silveira, J.A., Morales-Ojeda, S.M., 2014.
356 Trace element geochemistry of groundwater in a karst subterranean estuary (Yucatan
357 Peninsula, Mexico). Geochimica et Cosmochimica Acta 132, 31-49.
358 Gonneea, M.E., Morris, P.J., Dulaiova, H., Charette, M.A., 2008. New perspectives on radium
359 behavior within a subterranean estuary. Marine Chemistry 109, 250-267.
360 Gonneea, M.E., Mulligan, A.E., Charette, M.A., 2013a. Climate-driven sea level anomalies
361 modulate coastal groundwater dynamics and discharge. Geophysical Research Letters 40,
362 2701-2706.

363 Gonneea, M.E., Mulligan, A.E., Charette, M.A., 2013b. Seasonal cycles in radium and barium
364 within a subterranean estuary: Implications for groundwater derived chemical fluxes to
365 surface waters. Geochimica et Cosmochimica Acta 119, 164-177.
366 Klinkhammer, G.P., Palmer, M.R., 1991. Uranium in the oceans: Where it goes and why.
367 Geochimica et Cosmochimica Acta 55, 1799-1806.
368 Koide, M., Goldberg, E.D., 1963. Uranium-234/uranium-238 ratios in sea water. Progress in
369 Oceanography 3, 173-177.
370 Langmuir, D., 1978. Uranium solution-mineral equilibria at low temperatures with applications
371 to sedimentary ore deposits. Geochimica et Cosmochimica Acta 42, 547-569.
372 Maher, D.T., Eyre, B.D., 2010. Benthic fluxes of dissolved organic carbon in three temperate
373 Australian estuaries: Implications for global estimates of benthic DOC fluxes. Journal of
374 Geophysical Research: Biogeosciences 115.
375 Moore, W.S., 1999. The subterranean estuary: A reaction zone of ground water and sea water.
376 Marine Chemistry 65, 111-125.
377 Moore, W.S., 2008. Fifteen years experience in measuring 224Ra and 223Ra by delayed
378 coincidence counting. Marine Chemistry 109, 188-197.
379 Moore, W.S., Beck, M., Riedel, T., Rutgers van der Loeff, M., Dellwig, O., Shaw, T.J.,
380 Schnetger, B., Brumsack, H.J., 2011. Radium-based pore water fluxes of silica,
381 alkalinity, manganese, DOC, and uranium: A decade of studies in the German Wadden
382 Sea. Geochimica et Cosmochimica Acta 75, 6535-6555.
383 O'Connor, A.E., Luek, J.L., McIntosh, H., Beck, A.J., 2015. Geochemistry of redox-sensitive
384 trace elements in a shallow subterranean estuary. Marine Chemistry 172, 70-81.

385 Owens, S.A., Buesseler, K.O., Sims, K.W.W., 2011. Re-evaluating the 238U-salinity
386 relationship in seawater: Implications for the 238U-234Th disequilibrium method.
387 Marine Chemistry 127, 31-39.
388 Palmer, M.R., Edmond, J.M., 1993. Uranium in river water. Geochimica et Cosmochimica Acta
389 57, 4947-4955.
390 Rodellas, V., Garcia-Orellana, J., Tovar-Sánchez, A., Basterretxea, G., López-Garcia, J.M.,
391 Sánchez-Quiles, D., Garcia-Solsona, E., Masqué, P., 2014. Submarine groundwater
392 discharge as a source of nutrients and trace metals in a Mediterranean bay (Palma Beach,
393 Balearic Islands). Marine Chemistry 160, 56-66.
394 Roy, M., Martin, J.B., Cable, J.E., Smith, C.G., 2013. Variations of iron flux and organic carbon
395 remineralization in a subterranean estuary caused by inter-annual variations in recharge.
396 Geochimica et Cosmochimica Acta 103, 301-315.
397 Roy, M., Martin, J.B., Cherrier, J., Cable, J.E., Smith, C.G., 2010. Influence of sea level rise on
398 iron diagenesis in an east Florida subterranean estuary. Geochimica et Cosmochimica
399 Acta 74, 5560-5573.
400 Roy, M., Rouxel, O., Martin, J.B., Cable, J.E., 2012. Iron isotope fractionation in a sulfide
401 bearing subterranean estuary and its potential influence on oceanic Fe isotope flux.
402 Chemical Geology 300-301, 133-142.
403 Sadat-Noori, M., Santos, I.R., Sanders, C.J., Sanders, L.M., Maher, D.T., 2015. Groundwater
404 discharge into an estuary using spatially distributed radon time series and radium
405 isotopes. Journal of Hydrology 528, 703-719.

406 Sanders, C.J., Santos, I.R., Barcellos, R., Silva Filho, E.V., 2012. Elevated concentrations of
407 dissolved Ba, Fe and Mn in a mangrove subterranean estuary: Consequence of sea level
408 rise? Continental Shelf Research 43, 86-94.
409 Sanders, C.J., Santos, I.R., Maher, D.T., Sadat-Noori, M., Schnetger, B., Brumsack, H.J., 2015.
410 Dissolved iron exports from an estuary surrounded by coastal wetlands: Can small
411 estuaries be a significant source of Fe to the ocean? Marine Chemistry 176, 75-82.
412 Santos, I.R., Burnett, W.C., Misra, S., Suryaputra, I.G.N.A., Chanton, J.P., Dittmar, T., Peterson,
413 R.N., Swarzenski, P.W., 2011. Uranium and barium cycling in a salt wedge subterranean
414 estuary: The influence of tidal pumping. Chemical Geology 287, 114-123.
415 Santos, I.R., Machado, M.I., Niencheski, L.F., Burnett, W., Milani, I.B., Andrade, C.F.F.,
416 Peterson, R.N., Chanton, J., Baisch, P., 2008. Major ion chemistry in a freshwater coastal
417 lagoon from Southern Brazil (Mangueira Lagoon): Influence of groundwater inputs.
418 Aquatic Geochemistry 14, 133-146.
419 Santos, I.R., Peterson, R.N., Eyre, B.D., Burnett, W.C., 2010. Significant lateral inputs of fresh
420 groundwater into a stratified tropical estuary: Evidence from radon and radium isotopes.
421 Marine Chemistry 121, 37-48.
422 Swarzenski, P.W., 2007. U/Th series radionuclides as coastal groundwater tracers. Chemical
423 Reviews 107, 663-674.
424 Swarzenski, P.W., Baskaran, M., 2006. Uranium distribution in the coastal waters and pore
425 waters of Tampa Bay, Florida. Marine Chemistry 102, 252-266.
426 Tissot, F.L.H., Dauphas, N., 2015. Uranium isotopic compositions of the crust and ocean: Age
427 corrections, U budget and global extent of modern anoxia. Geochimica et Cosmochimica
428 Acta 167, 113-143.

429 Windom, H., Smith, R., Niencheski, F., Alexander, C., 2000. Uranium in rivers and estuaries of
430 globally diverse, smaller watersheds. Marine Chemistry 68, 307-321.

431

Table 1. A summary of SGD-derived U fluxes to the coastal ocean. Negative values represent a sink related to seawater recirculation in sediments.

Location	Site Description	Effective U endmember (nM)	SGD rate (L m^{-2} d^{-1})	U SGD flux (umol m^{-2} d^{-1})	
Korogoro Creek, Australia[1]	Tidal estuary, quartz sands	3.8	469	1.8	This work
Korogoro Creek, Australia[2]	Tidal estuary, quartz sands	1.5	275	0.4	This work
Yucatan, Mexico	Karst	10	20-48*	0.2-0.4	(Gonneea et al. 2014)
Tampa Bay, Florida	Coastal bay, sands	13.2	8.3	0.11**	(Swarzenski and Baskaran 2006)
Waquoit Bay, USA	Coastal bay, quartz sands	-5.7	82***	-0.4	(Charette and Sholkovitz 2006)
North Inlet, USA	Saltmarsh tidal creek	-8	15	-0.2	(Duncan and Shaw 2003)
Turkey Point, USA	Quartz sand beach	-119	5****	-0.6	(Santos et al. 2011)
York River Estuary, USA	Estuary, coarse sands	-2.9	55	-0.16	(O'Connor et al. 2015)

* Fluxes originally reported in units of $m^{-3}m^{-1}d^{-1}$ converted assuming SGD occurs within 2 km from the shore along a shoreline of 1100 km

**Converted using Tampa Bay area of 1030 km^2

*** Converted from 30 m y^{-1}

**** Fresh SGD rate converted using a 200-m seepage face.

[1]Effective SGD based on the endmember zero salinity intercept using surface water samples (salinity >30).

[2]SGD rate based on the fresh groundwater (salinity <2).

Table 2. A summary of the contribution of key coastal sources and sinks to oceanic budgets. Negative values represent a sink. The contribution of SGD remains unresolved due to large variability in fluxes in the systems investigated.

	U mol yr^{-1}	**Source**
Rivers	3 to 6 × 10^7	(Palmer and Edmond, 1993)
Saltmarsh	-3 × 10^7	(Windom et al., 2000)
SGD[1]	-5.4 × 10^7 to -1.3 × 10^9	This work
SGD[2]	6.8 × 10^6 to 1.7 × 10^8	This work

[1]Assumes global U endmember in SGD is the overall average of the seven sites shown in Table 1 (-15.5 nM).
[2]Excludes Turkey point from global average to obtain a U endmember of 1.7 nM.

493 **CAPTIONS TO FIGURES**

494

495 **Figure 1.** Study area. The blue circle indicates the beach times series measurement site, the grey
496 circles the 2D transect, the red circles represent the deep groundwater stations while the shallow
497 wells are indicated by green circles. White square indicates site of surface water measurements
498 in Sanders et al. (2015).

499

500 **Figure 2.** Contour plots of the beach time series measurements in a vertical transect at the low
501 tide mark sampled every 1 to 2 hours (see Supplement Material for more information on
502 sampling times).

503

504 **Figure 3.** Contour plots of the 2D groundwater transect along the sand beach STE.

505

506 **Figure 4.** Uranium groundwater metal concentrations in relation to iron, manganese, barium,
507 depth, dissolved organic carbon (DOC), pH and dissolved oxygen (DO %). The blue circle
508 indicates times series measurement site, the grey circles the 2D transect, the red circles represent
509 the deep groundwater stations while the shallow wells are indicated by green circles. Red circle
510 indicates obvious dissolved Fe outlier.

511

512 **Figure 5.** Salinity corrected U Groundwater values (U/sal ratios) used to correct for the effect of
513 dilution. The blue circle indicates times series measurement site, the grey circles the 2D transect,
514 the red circles represent the deep groundwater stations while the shallow wells are indicated by
515 green circles. Obvious dissolved Fe outlier shown in Figure 3 not included in this graph.

516

Figure 6. Uranium groundwater and surface water vs salinity in the groundwater and surface water samples. Surface water time series data is taken from Sanders et al., 2015. A theoretical mixing line is drawn by joining the creek and sea water end member assuming conservative mixing. The enlarged diagram is from the surface water salinities >30. The zero salinity intercept (3.8 nM) is estimated from these surface water samples only, and used to estimate the apparent net fluxes out of the STE.

Figure 7. Conceptual model showing the dissolved uranium export rates from the sandy beach subterranean estuary in this work.

Figure 1.

Figure 2.

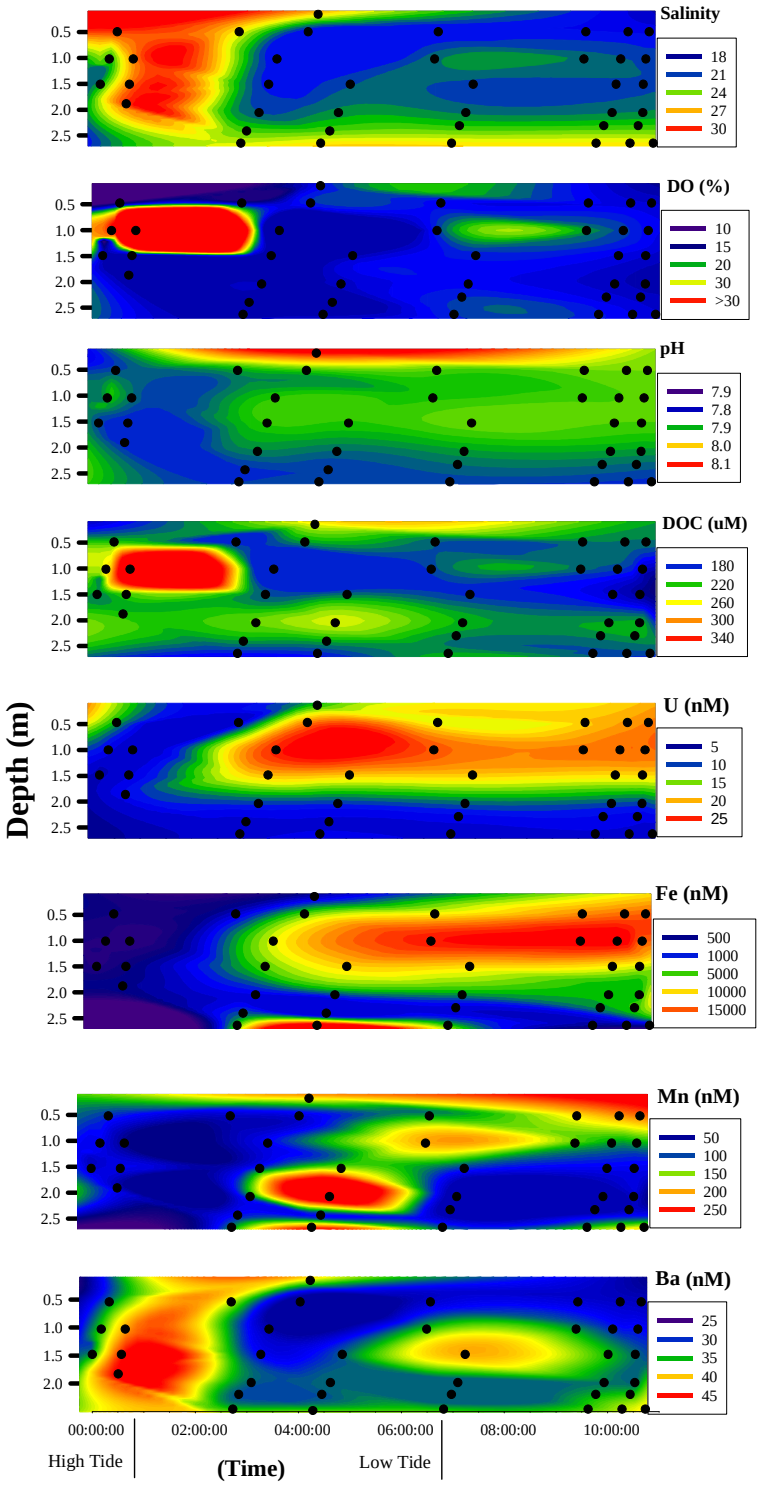
Salinity
18
21
24
27
30
DO (%)
10
15
20
30
>30
pH
7.9
7.8
7.9
8.0
8.1
DOC (uM)
180
220
260
300
340
U (nM)
5
10
15
20
25
Fe (nM)
500
1000
5000
10000
15000
Mn (nM)
50
100
150
200
250
Ba (nM)
25
30
35
40
45
Depth (m)
0.5
1.0
1.5
2.0
2.5
00:00:00
02:00:00
04:00:00
06:00:00
08:00:00
10:00:00
High Tide
(Time)
Low Tide

605
606 **Figure 3.**

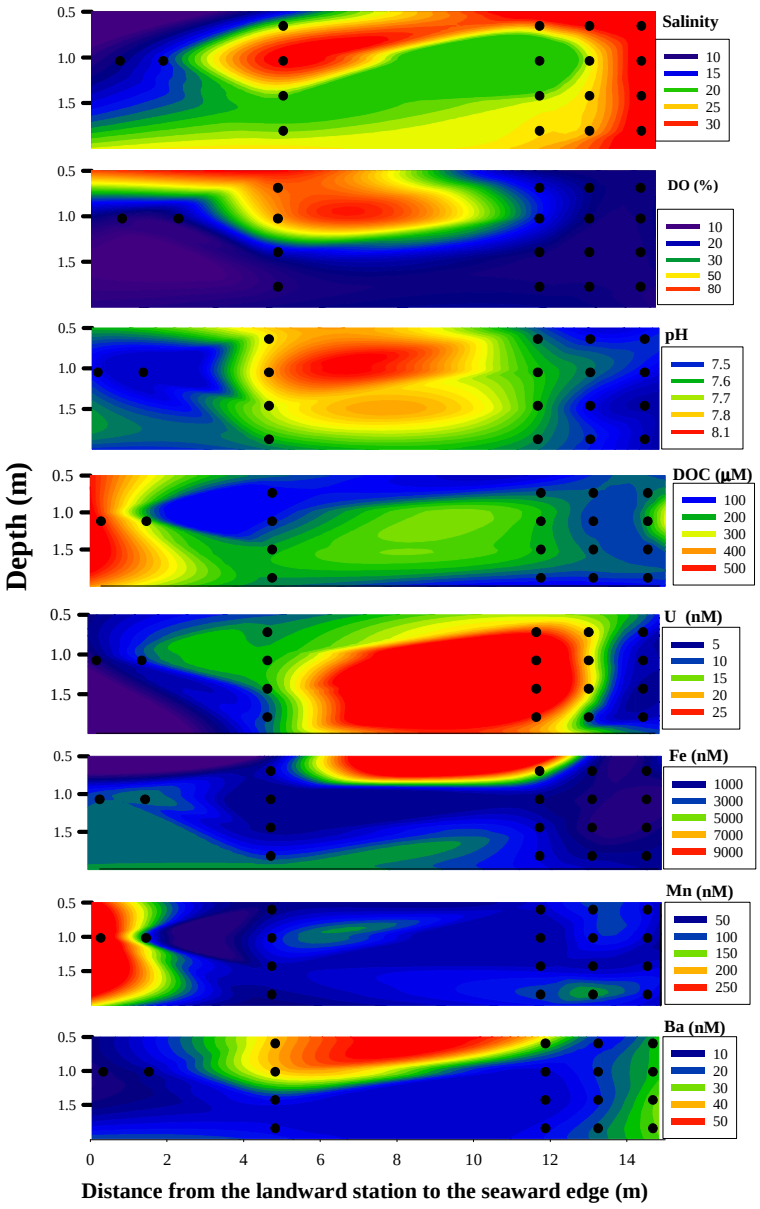

607

608 **Figure 4.**

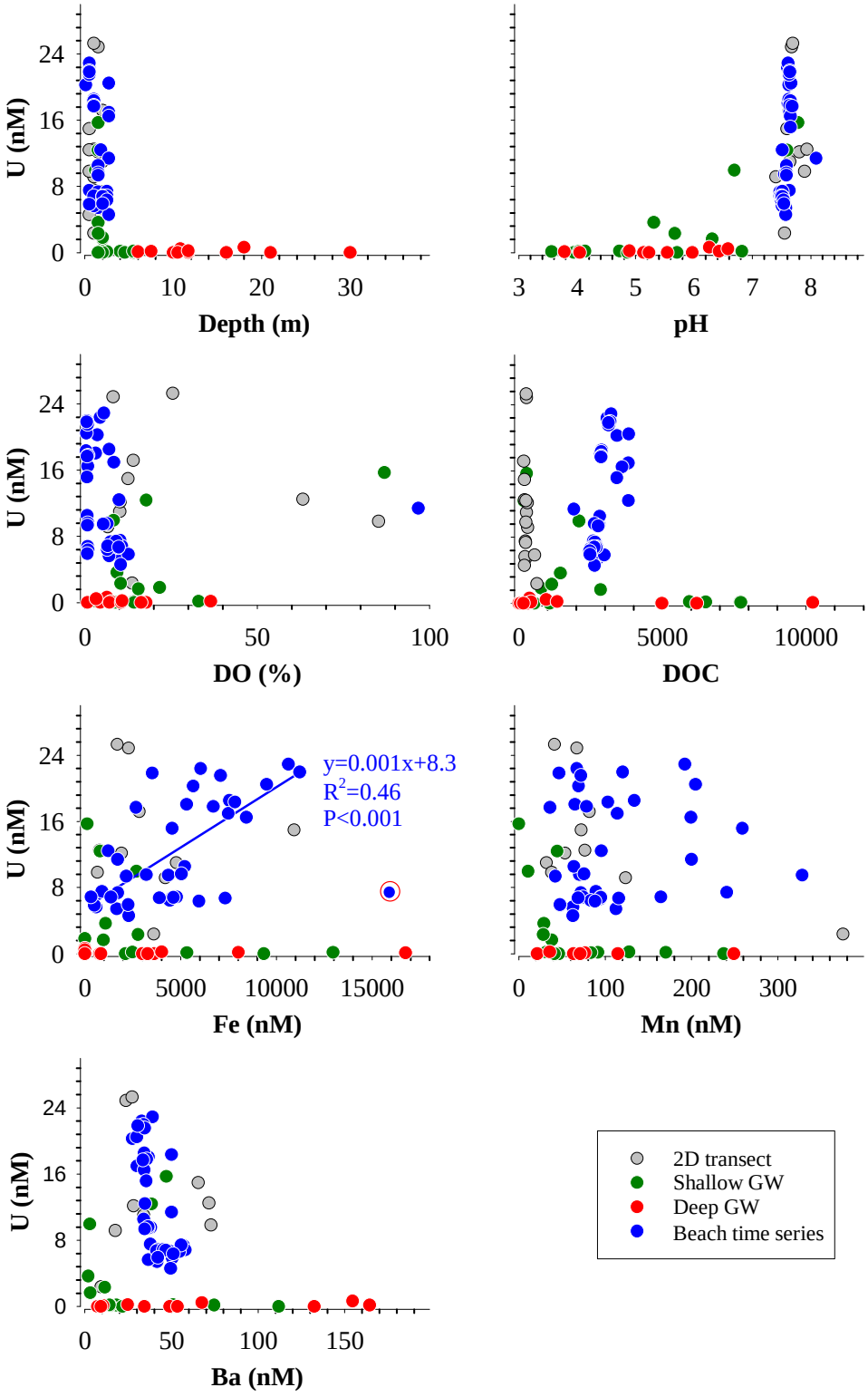

609

610 **Figure 5.**
611

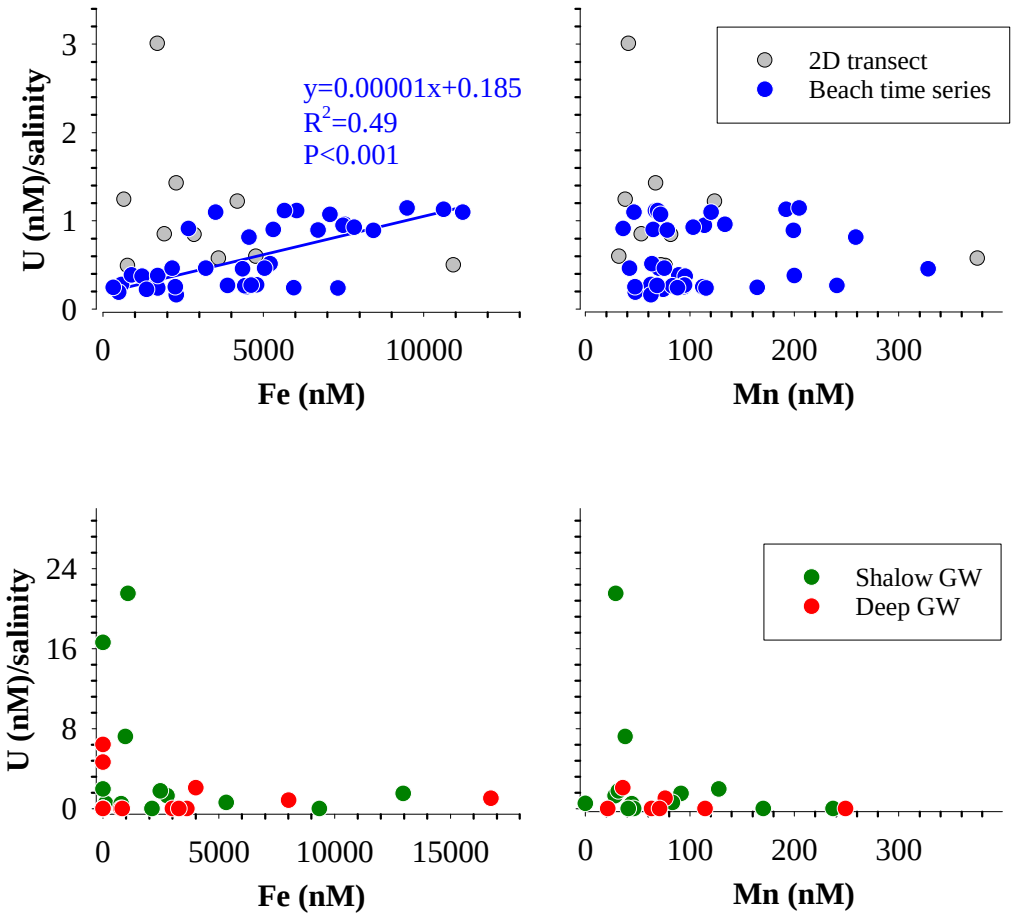

612
613
614
615
616
617
618
619
620
621
622
623
624
625
626
627
628

Figure 6.

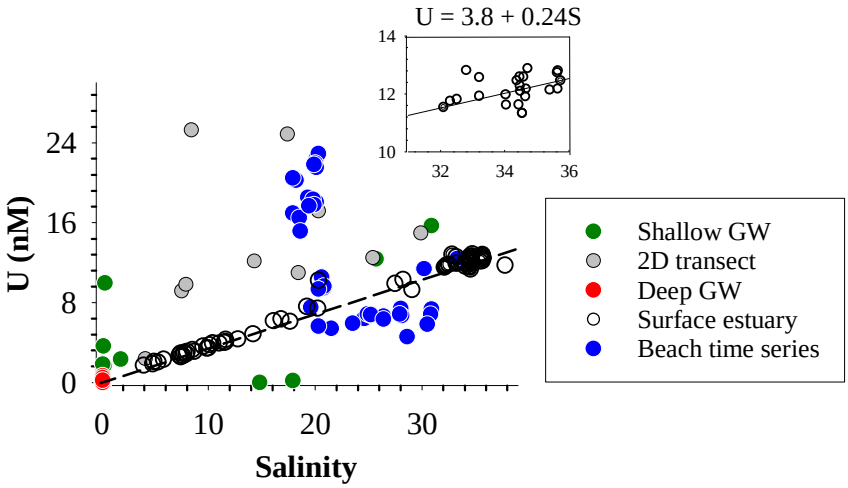

661 **Figure 7.**

662

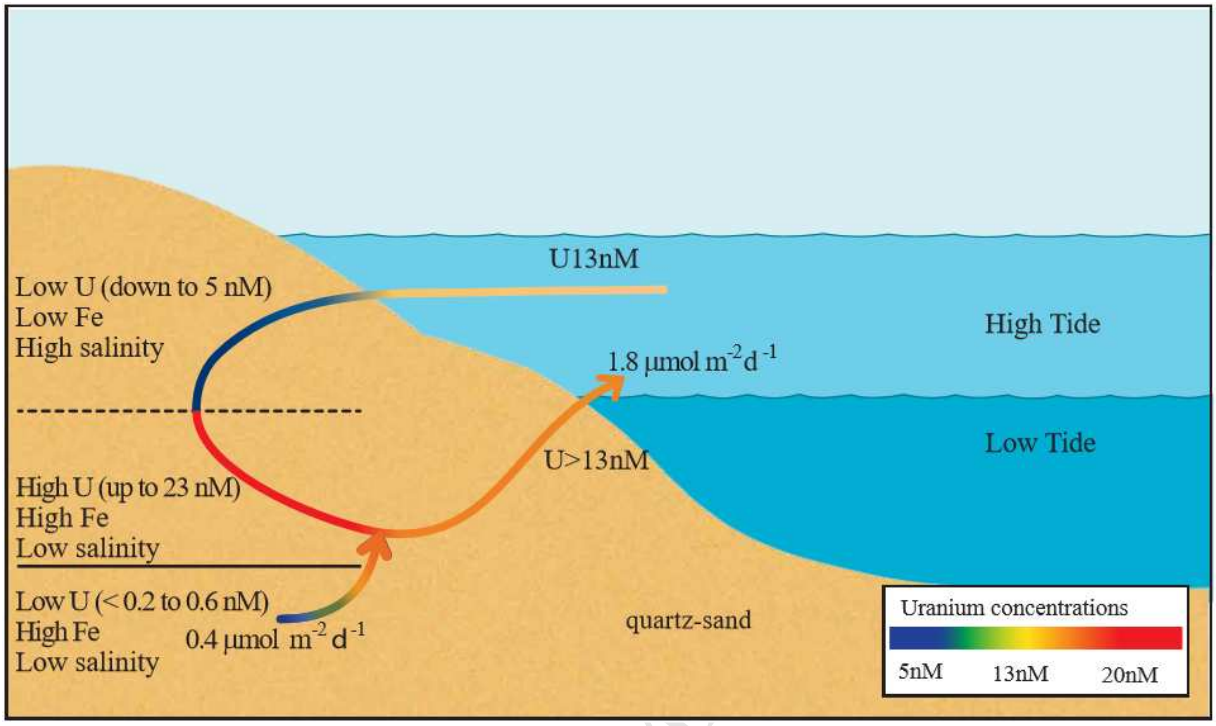

663